Integrative and Comparative Biology

Integrative and Comparative Biology, volume 57, number 1, pp. 103–111
doi:10.1093/icb/icx041

Society for Integrative and Comparative Biology

SYMPOSIUM

Scaling from Metabolism to Population Growth Rate to Understand How Acclimation Temperature Alters Thermal Performance

Thomas M. Luhring[1] and John P. DeLong

School of Biological Sciences, University of Nebraska, Lincoln, NE 68588, USA

From the symposium "Indirect Effects of Global Change: from Physiological and Behavioral Mechanisms to Ecological Consequences (SICB wide)" presented at the annual meeting of the Society for Integrative and Comparative Biology, January 4–8, 2017 at New Orleans, Louisiana.

[1]E-mail: tomluhring@gmail.com

Synopsis The mean and variance of environmental temperature are changing as a consequence of human activities. Ectotherms are sensitive to these temperature changes in the short term, typically displaying a unimodal response of most biological rates to temperature (thermal performance curves; TPCs). Many organisms, however, may acclimate or evolve in response to new temperature regimes. In particular, population growth rate TPCs (*r* TPCs) reflect the ability to maintain positive growth under a range of temperatures, and therefore shifts in *r* TPCs due to acclimation are fundamental to our understanding of how ectotherms will respond to changes in climate. Here, we derive a model for *r* TPCs rooted in temperature dependent metabolic rate (through enzyme kinetics and activity). We then use this model to interpret the effects of acclimation to different temperatures on *r* TPCs of the protist *Paramecium bursaria*. Intermediate acclimation temperatures generally resulted in higher upper critical thermal limits, thermal optima, maximum population growth rate, and the area under the TPC. Lower critical thermal limits increased linearly with acclimation temperature, causing a decrease in thermal breadth with increased acclimation temperature. Thus, rather than showing improved performance at the acclimation temperature, *P. bursaria* appeared to pay a price at all temperatures for acclimating to higher temperatures. The fits of our data to our model also suggest that changes in the structure and function of metabolic enzymes may underlie the changes in the TPCs. Specifically, our results suggest that both the delta heat capacity and delta enthalpy of formation of metabolic enzymes may have increased with acclimation. Since these two factors are correlated across acclimation temperatures, our data also suggest potential trade-offs that may constrain changes in TPCs.

Introduction

The biology of ectotherms is largely controlled by temperature-dependent phenomena (Hochachka and Somero 2002; Brown et al. 2004; Kingsolver 2009). Temperature-dependent processes are often characterized by unimodal thermal performance curves (TPCs) that describe the change in biological rates and traits across a range of temperatures (Scheiner 2002; Angilletta 2009; Kingsolver 2009). TPCs for population growth rate (*r*) are particularly crucial, as they are a measure of the temperature dependence of fitness and may predict how organisms will respond to changing climatic conditions (Charlesworth 1994; Deutsch et al. 2008; Bozinovic et al. 2011; Clusella-Trullas et al. 2011; Amarasekare and Savage 2012; Kingsolver et al. 2013; Vasseur et al. 2014). The shapes of *r* TPCs vary among and within species as a result of differences in acclimation, predation risk, genetics, and latitude (Izem and Kingsolver 2005; Pörtner and Knust 2007; Angilletta 2009; Clusella-Trullas et al. 2011; Luhring and DeLong 2016).

Although many biological processes change in a continuous nonlinear manner across temperature, acclimation studies often compare the effects of acclimation treatments within a limited set of temperature treatments instead of the entire TPC (e.g., Leroi et al. 1994). We argue that acclimation and other factors that change temperature-dependent performance should be measured across the entirety of an organism's thermal tolerance breadth to understand how they change the shape of the TPC for that metric (e.g., Padfield et al. 2016). Furthermore, the parameters used to describe how TPCs change need to be

Advanced Access publication June 28, 2017

rooted in biologically meaningful processes (an oft repeated plea regarding the use of TPCs; Schulte et al. 2011; Schulte 2015). There is a substantial bestiary of models to describe the shapes of population growth TPCs (Krenek et al. 2011), however these models are often phenomenological in nature instead of being derived from biologically meaningful processes. Thus, when comparing TPCs, we are often limited to comparing model parameters with no clear biological meaning or the emergent properties of the curves themselves (e.g., optimal temperatures, critical upper and lower temperatures). Furthermore, because population declines occur beyond upper and lower critical temperature limits, models for population growth rate TPCs must be able to go negative beyond upper and lower critical limits—a critical shortcoming of some popular models (e.g., Ratkowsky et al. 2005; Gaussian-quadratic function in Deutsch et al. 2008). A model with biologically meaningful parameters is needed to understand the biological underpinnings of changes to population growth rate TPCs that result from adaptation to changing climates or shifts in ecological context.

To create a more mechanistic model tying population growth rate to temperature, we link maximum population growth rate (r_{max}) to temperature dependent metabolic rate. To do this, we build on the ideas that (1) metabolic rate is a temperature-dependent process determined by the combined effects of temperature on enzyme stability and reactant kinetics (DeLong et al. 2017), (2) biomass production is fueled by metabolism (Verity 1985; Ernest et al. 2003; DeLong and Hansen 2009), and (3) reproduction is limited by biomass production. Thus, population growth rate depends on biomass production, biomass production depends on metabolism, and metabolic rate depends on temperature-dependent processes (reviewed in Brown et al. 2004; Brown and Sibly 2006). Even though organisms vary in the proportion of metabolism devoted to biomass production, maintenance, and individual growth, the temperature- and body size-dependence of biomass production follows closely the temperature- and body size dependence of metabolic rate, suggesting a strong link between metabolic rate and production (Ernest et al. 2003).

Although there are several potential metabolic rate models from which to base a population growth rate model, most fail to meet critical biological assumptions in their derivation (see Table 1 in DeLong et al. 2017). In contrast, the recently developed enzyme-assisted Arrhenius (EAAR) model casts the unimodal dependence of metabolic rate on temperature as arising from the effects of temperature on enzyme kinetics and protein stability (DeLong et al. 2017). The EAAR model builds on the Arrhenius equation by allowing enzymes to lower the activation energy of metabolic reactions. If instead of an overall activation energy, we define a baseline energetic hurdle for a reaction to proceed independent of enzymatic

Table 1 Bootstrapped estimates of parameter means with 95% upper and lower confidence limits (LCL and UCL) for *Paramecium bursaria* population growth rate (*r*) thermal performance curves across four acclimation treatments

Parameter	Acclimation	Mean	LCL	UCL
E_b	10	0.03[a]	NA	NA
	19	0.03	0.01	0.04
	23	0.03	0.02	0.04
	28	0.04	0.02	0.08
$E_{\Delta H}$	10	1.08	0.63	1.40
	19	1.55	0.90	2.07
	23	1.74	1.23	2.20
	28	2.42	1.43	4.92
$E_{\Delta Cp}$	10	0.10	0.03	0.15
	19	0.15	0.07	0.21
	23	0.17	0.10	0.24
	28	0.31	0.17	0.57
T_m	10	308.29	305.72	317.06
	19	309.02	307.88	311.91
	23	309.45	307.41	312.51
	28	304.77	303.80	305.77
T_{min}	10	286.38	282.74	289.18
	19	288.37	286.45	289.92
	23	288.91	287.21	290.46
	28	289.54	288.07	290.90
Breadth	10	21.91	17.88	33.91
	19	20.64	18.13	25.01
	23	20.54	17.27	25.23
	28	15.23	13.46	17.20
T_{opt}	10	297.23	295.58	300.14
	19	298.57	297.66	299.59
	23	299.09	298.33	299.91
	28	297.11	296.29	297.81
P_{max}	10	0.34	0.26	0.43
	19	0.56	0.51	0.63
	23	0.56	0.50	0.63
	28	0.46	0.38	0.53
AUC	10	3.12	2.30	4.56
	19	4.55	3.89	5.65
	23	4.32	3.71	5.07
	28	2.57	1.93	3.10

Note: T_m, T_{min}, and T_{Opt} are in Kelvins; and AUC, area under the curve.

[a]E_b in for the 10 °C acclimation treatment was fixed at 0.03 (see "Methods and materials" section).

contributions as E_b and then define a lowering of that activation energy through the contributions of enzymes, E_c, we can rewrite the Arrhenius equation as

$$R = A_0 e^{\frac{-(E_b - E_c)}{kT}}. \quad (1)$$

The contribution of enzymes to lowering the activation energy is temperature dependent because enzyme stability and activity are temperature dependent, a fact that has been recognized by several previous efforts to derive TPCs for enzyme-catalyzed reactions (Johnson and Lewin 1946; Sharpe and DeMichele 1977; Schoolfield et al. 1981; Hobbs et al. 2013). We then use the Becktel–Shellman equation for free energy (Becktel and Schellman 1987) to model the activity of the catalyzing enzymes as a function of temperature

$$\Delta G = \Delta H\left(1 - \frac{T}{T_m}\right) + \Delta C_p\left(T - T_m - T\ln\frac{T}{T_m}\right), \quad (2)$$

where ΔH is the enthalpy of folding the enzymes used in the metabolic reaction, relative to the melting temperature, T_m, and ΔC_p is the difference in heat capacity between the folded and unfolded state of the enzymes, again relative to the melting temperature. ΔG reflects the stability of the enzyme, and critically, the probability of an enzyme being in an active state and able to lower the reaction's activation energy (Ratkowsky et al. 2005; Feller 2010; Hobbs et al. 2013). The free energy of the catalyst, however, does not equal the reduction in the activation energy but rather indicates the probability that the catalyzing enzymes are in active state. This probability approaches 1 at the maximum ΔG, so we rescale Equation (2) by the maximum free energy, ΔG_{max}, to transform it into a probability between 0 and 1. Finally, given activity, the catalyst lowers the activation energy by an amount E_L, such that $E_c = E_L \frac{\Delta G}{\Delta G_{max}}$. Thus, we replace each parameter in Equation (2) to account for this transformation (i.e., $E_{\Delta H} = E_L \frac{\Delta H}{\Delta G_{max}}$, $E_{\Delta Cp} = E_L \frac{\Delta C_p}{\Delta G_{max}}$) and rewrite Equation (2) as

$$E_c = E_{\Delta H}\left(1 - \frac{T}{T_m}\right) + E_{\Delta Cp}\left(T - T_m - T\ln\frac{T}{T_m}\right). \quad (3)$$

Substituting Equation (3) into Equation (2), we get

$$R = A_0 e^{\frac{-\left(E_b - \left(E_{\Delta H}\left(1 - \frac{T}{T_m}\right) + E_{\Delta Cp}\left(T - T_m - T\ln\frac{T}{T_m}\right)\right)\right)}{kT}}, \quad (4)$$

which now provides a mechanistic description of the temperature dependence of metabolic rate that is generated by both reactant kinetics and temperature-dependent enzyme stability. Although not all biomass production is allocated to reproduction, all reproduction is created from newly produced biomass and thus is inextricably linked to metabolism. If reproduction is proportional to biomass production, and biomass production is proportional to metabolism, then we can define a birth function b by creating a new constant (B_0) that combines with A_0 to convert metabolism into production into births

$$b = B_0 e^{\frac{-\left(E_b - \left(E_{\Delta H}\left(1 - \frac{T}{T_m}\right) + E_{\Delta Cp}\left(T - T_m - T\ln\frac{T}{T_m}\right)\right)\right)}{kT}}. \quad (5)$$

In this simple derivation, births are only temperature dependent as a function of biomass production. However, the total number of individuals produced per unit of biomass can vary with temperature, which would require an additional temperature dependent function to be included in the constant B_0. Here, we focus on the simplest scenario because we are working with a type of organism where all production is reproduction (protists), but we recognize that Equation (5) may need to be altered for other types of organisms. Although survival also may be linked to metabolism, empirically it appears that death rates are related to temperature through an Arrhenius-type function, where mortality increases exponentially with temperature (Savage et al. 2004; Amarasekare and Savage 2012). Thus, we can write a death function d as:

$$d = D_0 e^{\frac{-E_b}{kT}}.$$

Although we use the same parameters (k and E_b) as previous iterations of the Arrhenius function for death rate, we caution that the underlying mechanism for their apparent similarity is not known and this part of the model remains as a phenomenological placeholder for future development of a mechanistic death function. Population growth is the sum of factors increasing population size (birth and immigration) and factors decreasing population size (death and emigration). For this model, we ignore the movement of individuals into or out of a population and instead focus solely on vital rates (birth and death) across temperature. Although a general framework for the dependence of population growth on temperature exists for age-structured populations (Amarasekare and Savage 2012), we focus on a simpler setup in order to emphasize the link between metabolism and overall reproduction. Thus, we focus the initial derivation of r as the difference between

death and birth rates and write a full population growth TPC as

$$r = B_0 e^{\frac{-\left(E_b - \left(E_{\Delta H}\left(1-\frac{T}{T_m}\right) + E_{\Delta Cp}\left(T - T_m - T\ln\frac{T}{T_m}\right)\right)\right)}{kT}} - D_0 e^{\frac{-E_b}{kT}}. \quad (7)$$

We use Equation 7 (the *r*-EAAR model) to interpret variation in population growth TPCs for the protist *Paramecium bursaria* acclimated to different temperatures. Fitted parameters of the *r*-EAAR model are rooted in the properties of enzyme populations, permitting us to infer potential changes in enzyme thermodynamics caused by acclimation treatments.

Methods and materials

Study species rearing and maintenance

We isolated *P. bursaria* from a freshwater pond on the Spring Creek Prairie Audubon Center in southeastern Nebraska (Novich et al. 2014; Luhring and DeLong 2016). Isolated cells were grown in media made from a 1:9 ratio of liquid protozoa medium (Carolina Biological Supply, Burlington, NC, USA) to pond water (filtered 2× and autoclaved). The media was autoclaved and then bacterized with a mix of bacteria from the source pond (see Luhring and DeLong 2016 for details). Cultures of *P. bursaria* were kept in a constant state of semi-exponential growth through weekly water changes where part of the culture was added to a new batch of bacterized media. Cultures were maintained on a 12:12 h light:dark cycle at 21°C in growth chambers (Percival, Fontina, WI, USA).

Acclimatization and performance trials

Prior to performance trials, *P. bursaria* were acclimated to one of five acclimation temperatures (10, 19, 23, 28, or 35°C) for 48 h in 90-mm Petri dishes ($n = 75$ initial population for each 150 mm dish, four 150 mm dishes per acclimation temperature). Acclimation temperatures were chosen to include a full range of temperatures from below to above the lower and upper critical temperatures, respectively. Because of high mortality in the 35°C acclimation, we dropped that treatment from analyses and only report data from the lower four acclimation temperatures. After acclimation, six *P. bursaria* from acclimated populations were placed into each of six 60 mm petri dishes for each of the nine performance trial temperatures (10, 19, 21, 23, 25, 28, 30, 32, 35°C) ($n = 36$ *P. bursaria* per temperature). Because of limitations with the availability of environmental chambers, three groups of trials were run on October 9, 2015 (10 and 28°C acclimations at 10, 21, 25, 28, 30, 32, 35°C), November 6, 2015 (19 and 23°C acclimations at 10, 19, 21, 23, 28, 32, 35°C), and January 29, 2016 (10 and 28°C acclimations at 19, 23°C; 19 and 23°C acclimations to 25, 30°C) to accomplish all acclimation by performance temperature combinations ($n = 36$).

Population growth rate (*r*)

Cells in each dish were counted every 24 h. Each estimate of population size (N_t) was the average of three replicate counts. Population growth rate was calculated over 48 h as $N_t = N_0 e^{rt}$, where N_0 is the population size at the beginning of the experiment (six cells) and N_t is the population size at 48 h. Because resources were nonlimiting in the short trial and population sizes of *P. bursaria* increased exponentially for the first 48 h (T.M.L. and J.P.D. unpublished data), the estimated *r* is approximately r_{max}.

Curve-fitting and statistical analyses

We fit the equation for the *r*-EAAR model (Equation [7]) to r_{max} values across the nine performance trial temperatures for each of the four acclimation temperatures using the fit function in MatLab (R2015b). We conducted the fitting in two stages. First, we estimated T_m by fitting a quadratic equation to the portion of the data to the right of and including the peak values. We did this because of potential structural correlations within Equation (7) that weaken our ability to fit T_m along with the other parameters. Second, using the T_m estimated in stage one, we fix T_m in Equation (7) and fit the equation to the data to estimate the remaining parameters. We used 1000 bootstrapped samples in both stages to estimate mean and 95% confidence intervals for the model parameters ($E_{\Delta Cp}$, $E_{\Delta H}$, E_b, T_m). TPC bootstraps for the coldest acclimation temperature were fitted with a fixed E_b of 0.03 (E_b for 19 and 23°C acclimations were 0.03) to prevent fitting artefacts that generated a negative value for E_b. Within each bootstrap iteration, we calculated five commonly used TPC characteristics and used the 2.5% and 97.5% quantiles across the bootstrapped fits as 95% confidence intervals for those characteristics. T_{min} is the temperature at which population growth crosses from negative to positive at low temperatures and was calculated by finding the lower x-intercept through the "vpasolve" numeric solver in MatLab. TPC Breadth was then calculated as $T_m - T_{min}$. The area under the TPC area under the curve (AUC) was calculated by integration of the curve between T_{min} and T_m using "integral" in MatLab. T_{opt} was found by solving for where the slope of the curve between T_{min} and T_m was 0. The value for *r* at T_{Opt} was then calculated to provide P_{max}.

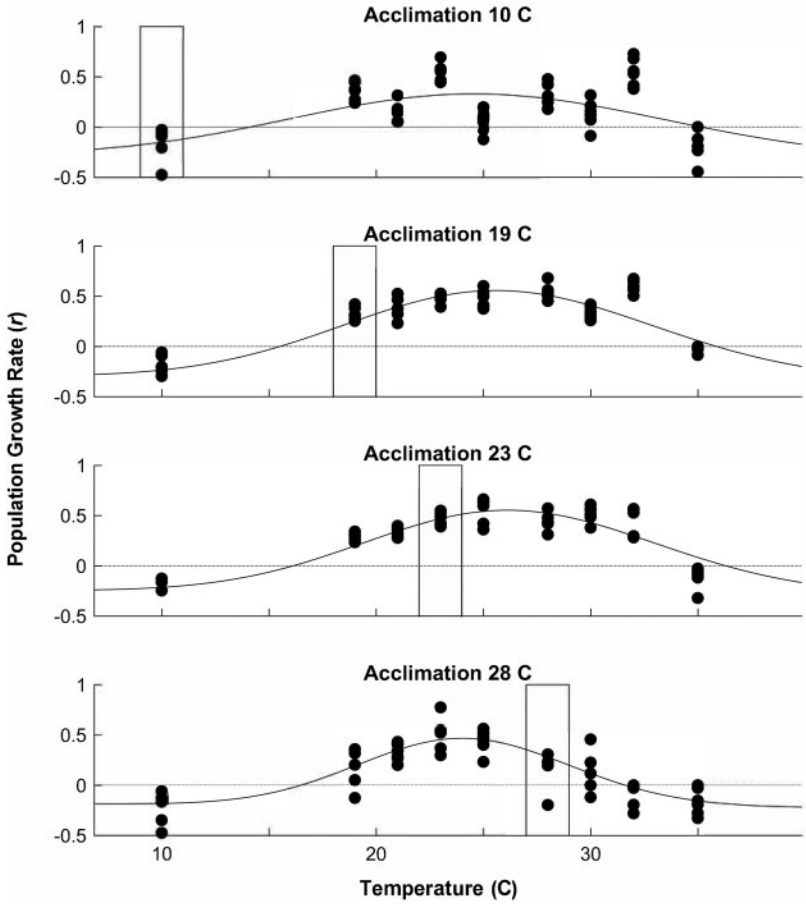

Fig. 1 Population growth rate (*r*) TPCs of *P. bursaria* acclimated to (from top to bottom) 10, 19, 23 and 28 °C for 48 h. A black box indicates the acclimation temperature of *P. bursaria* within each acclimation TPC. Curves depict *r* TPCs using mean bootstrapped parameter estimates. Each dot shows the population growth rate of a replicate dish of *P. bursaria* over 48 h from an initial population of six individuals. Temperature shown is in Celsius for ease of interpretation although TPCs were characterized in Kelvins.

Results

Regardless of acclimation treatment, no replicates in the 10 or 35°C performance trials had positive population growth over the 48-h period. This indicates that the resulting TPCs characterize *r* over the entire range of temperatures for which population growth is generally positive in *P. bursaria*. Although *P. bursaria* acclimated to 10, 19 and 23°C all had positive *r* in 32°C performance trials, those acclimated at 28°C showed zero or negative growth at that temperature (Fig. 1). Only *P. bursaria* acclimated at the lower (10°C) and upper (28°C) ends of their thermal tolerances demonstrated negative population growth at any of the intermediate temperatures (19–32°C).

Most fitted parameters ($E_{\Delta Cp}$, $E_{\Delta H}$) increased with acclimation temperature (Fig. 2; Table 1). However, enzyme melting temperature (T_m) was highest when acclimated at intermediate temperatures and lowest in those acclimated to higher temperatures. Although E_b was only estimated for the three warmest acclimation temperature treatments, it did not appear to show much change (0.03–0.04).

Most TPC properties, including T_{opt}, P_{max}, and the area under the TPC (AUC), were higher at intermediate acclimation temperatures than at the hotter and colder acclimation temperatures, indicating greater overall performance at intermediate temperatures (Fig. 2; Table 1). In contrast, T_{min} increased with acclimation temperature, leading to a decrease in TPC breadth with acclimation temperature.

Discussion

The ability to make physiological adjustments is central to an organism's ability to tolerate variation in environmental conditions. Our theory-data analysis indicates that *P. bursaria* population growth rate TPCs can shift when acclimated to different temperatures across their range of thermal tolerance. Nearly all fitted parameters and TPC properties changed across acclimation temperatures, with the general

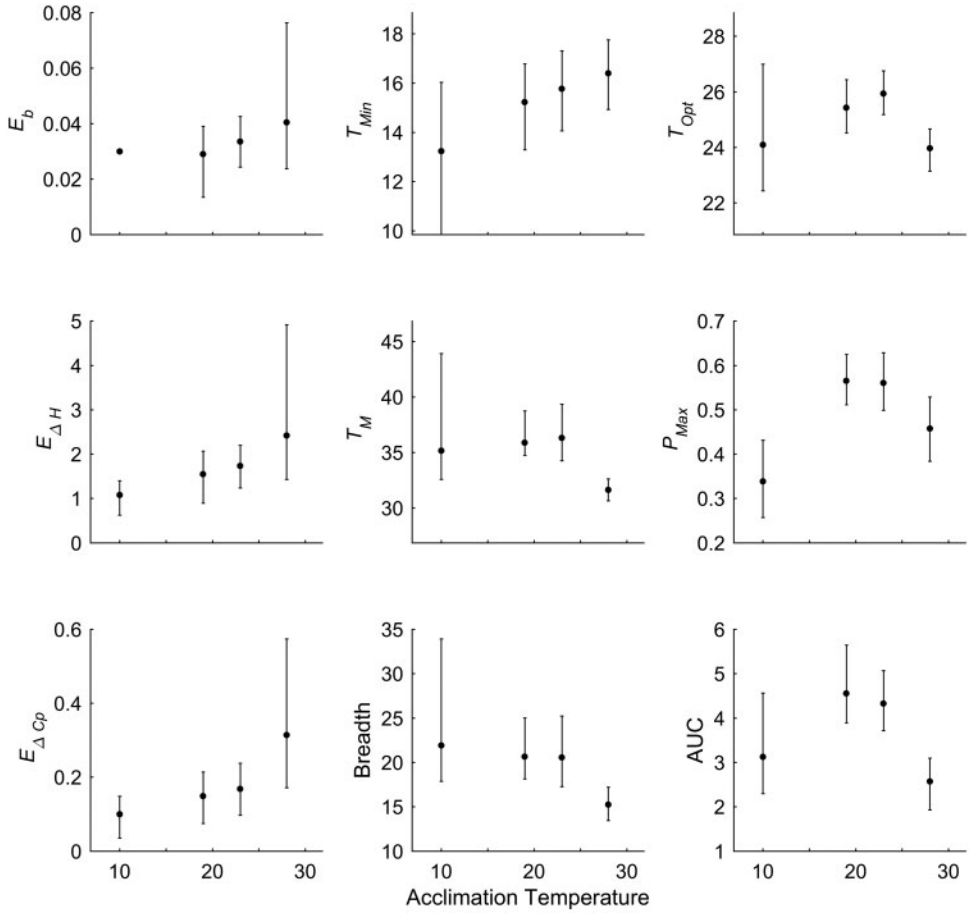

Fig. 2 Bootstrapped estimates with 95% confidence limits of fitted parameters (E_b, $E_{\Delta Cp}$, $E_{\Delta H}$, T_M) and TPC characteristics (T_{min}, Breadth, T_{opt}, P_{max}, AUC) across acclimation temperatures. Temperature shown is in Celsius for ease of interpretation although TPCs were characterized in Kelvins.

outcome that intermediate acclimation temperatures were associated with higher overall performance (T_m, T_{opt}, P_{max}, and the area under the TPC). This is generally consistent with previous work that suggests acclimation to intermediate temperatures is more beneficial across all temperatures than acclimation to relatively high or low temperatures (Zamudio et al. 1995). However, not all metrics of "better" were better at intermediate temperatures. For example, *P. bursaria* acclimated to the coldest temperature showed the lowest T_{min} and a T_m and a thermal breadth similar to cells acclimated to intermediate temperatures.

One potential benefit of using the *r*-EAAR model to interpret TPC data is that it points to potential changes in enzyme thermodynamics associated with changes in acclimation temperature. While we did not directly measure enzymatic properties, this potential link would be useful for elucidating the effects of molecular processes on higher-level functions. For instance, *P. bursaria* generally increased $E_{\Delta Cp}$ and $E_{\Delta H}$ with acclimation temperature, which would suggest that metabolically important enzymes could have higher energy content (greater enthalpy of formation) and be more resistant to temperature change (greater heat capacity) as acclimation temperatures increase. This could occur through a variety of mechanisms, including changes in the relative composition of enzymes, their thermal stability, or the employment of protective agents such as heat shock proteins. Although we did not directly measure heat capacity or enthalpy of the catalyzing enzymes, the shifts in $E_{\Delta Cp}$ and $E_{\Delta H}$ suggest that future work to understand how organism physiology changes in response to acclimation temperature could focus on the thermodynamic structure of enzymes associated with metabolism.

The *r*-EAAR model is a first step into expanding our understanding of how temperature dependent processes at the molecular level scale up through additional levels of organization (see DeLong et al. 2017). The model has important advantages over competing models that describe the thermal performance of population growth rate. First, the model is built on underlying mechanisms rather than shape characterization, as is the case for many competing models (see Krenek et al 2011, but see Amarasekare and

Savage 2012 for a general derivation). Specifically, our model uses metabolic processes to drive biomass production, allowing the factors that control the temperature dependence of metabolic reactions to scale up to population growth. Second, our model allows for both reasonable variation in shape and for negative population growth at high and low temperatures. There are several models currently in use that do not allow for negative growth at high and low temperatures, making these models suspect both in terms of their underlying mechanisms and in their ability to fully describe the TPC (e.g., Ratkowsky et al. 2005; Deutsch et al. 2008; Vasseur et al. 2014). For instance, these models would be exceptionally optimistic when projecting the effects of climate change variability and temperature warming for organisms with decreased thermal tolerance and or an increased T_{min} at warmer temperatures (both of which were seen with *P. bursaria* in this study). It is paramount to understand how physiology and climate interact to affect the abilities of organisms to persist through increasing mean temperature, temperature variability, and climatic extremes (Parmesan and Yohe 2003; Overpeck and Udall 2010; Vasseur et al 2014; Luhring and Holdo 2015).

P. bursaria meets key assumptions of our model, which may account for the ability of the model to describe changes in their r_{max} TPCs. *P. bursaria* reproduces by binary fission, making biomass production proportional to reproduction as assumed by our model. However, it may be important to incorporate deviations from these assumptions into future permutations of the *r*-EAAR model. Multicellular organisms that do not reproduce through binary fission may show differences in the temperature dependence of biomass production and fecundity through temperature dependent effects on clutch or offspring size. Furthermore, age-structured populations may show other temperature effects such as the temperature dependence of maturation (e.g., Amarasekare and Savage 2012). Such additional effects could be incorporated into our model as appropriate. Similarly, we used the Arrhenius function to make death rate a monotonically increasing function of temperature (Savage et al. 2004). But this is a phenomenological place-holder, and the Arrhenius function misses the potential for increasing death rates at colder temperatures, which also could be accommodated with other functions as needed.

We generally attribute the changes in *P. bursaria* *r*-TPCs observed here to phenotypic plasticity, given the relatively small number of generations that occurred during the experiment and the presumed low genetic diversity of the largely clonal stock populations. Although a variety of pathways may underlie the changes in the key parameters of $E_{\Delta Cp}$ and $E_{\Delta H}$, one interesting possibility is a change in heat-shock proteins (HSPs) (Pauwels et al. 2005). HSPs may buffer organisms against higher temperatures by preventing the denaturing of proteins, although the exact protein involved in tolerating higher temperatures varies among organisms, (e.g., Parsell et al. 1993). In our experiment, *P. bursaria* in the warmest acclimation treatment showed lower performance metrics across all temperatures. This could be related to temperature-dependent development (e.g., Wilson and Franklin 2002) or high amounts of HSPs lowering metabolic activity (e.g., Viant et al. 2003). Previous work demonstrates that other stressors such as predation also can induce the production of HSPs (Pauwels et al. 2005) or affect *r* TPCs (Luhring and DeLong, 2016). The commonality of HSP production for heat stress and predation exposure is interesting because the shift in the *r* TPC for *P. bursaria* under high temperature acclimation (Fig. 1) is similar to the shift in the *r* TPC for *P. aurelia* exposed to predation (Luhring and DeLong 2016). *P. aurelia* exposed to predation and *P. bursaria* exposed to higher acclimation temperatures showed reduced cold tolerances (increased T_{min}), decreased TPC breadths, and lowered T_{opt}. Thus, it may be worth looking into the role of HSPs in driving shifts in TPCs in response to a variety of environmental stressors. Furthermore, if HSPs influence both $E_{\Delta Cp}$ and $E_{\Delta H}$, they may function as a constraint generating trade-offs in TPC shape. Thus, future work focusing on the role of HSPs, or other candidate factors, may allow us to unravel how multiple simultaneous stressors will influence how organisms respond to future climate change.

Acknowledgments

T.M.L. thanks the University of Nebraska Program of Excellence in population ecology and the School of Biological Sciences. We thank R. Allen and R. Hruska for helping to run the experiment and count endless dishes of *Paramecium* and J. P. Gibert for comments and suggestions throughout the course of the experiment and analysis.

Funding

This work was supported by BSF [grant number 2014295 to J.P.D.], a McDonnell Foundation complex systems scholar award [to J.P.D.], and the University of Nebraska Program of Excellence in Population Biology postdoctoral fellowship [to T.M.L].

References

Amarasekare P, Savage V. 2012. A framework for elucidating the temperature dependence of fitness. Am Nat 179:178–91.

Angilletta MJ. 2009. Thermal adaptation: a theoretical and empirical synthesis. Oxford: Oxford University Press.

Becktel WJ, Schellman JA. 1987. Protein stability curves. Biopolymers 26:1859–77.

Bozinovic F, Bastías DA, Boher F, Clavijo-Baquet S, Estay SA, Angilletta MJ. 2011. The mean and variance of environmental temperature interact to determine physiological tolerance and fitness. Physiol Biochem Zool 84:543–52.

Brown JH, Gillooly JF, Allen AP, Savage VM, West GB. 2004. Toward a metabolic theory of ecology. Ecology 85:1771–89.

Brown JH, Sibly RM. 2006. Life-history evolution under a production constraint. Proc Natl Acad Sci U S A103:17595–9.

Charlesworth B. 1994. Evolution in age-structured populations. Cambridge: Cambridge University Press.

Clusella-Trullas S, Blackburn TM, Chown SL. 2011. Climatic predictors of temperature performance curve parameters in ectotherms imply complex responses to climate change. Am Nat 177:738–51.

DeLong JP, Gibert JP, Luhring TM, Bachman G, Reed B, Neyer A, Montooth KL. 2017. The combined effects of reactant kinetics and enzyme stability explain the temperature dependence of metabolic rates. Ecol Evol published online (doi:10.1002/ece3.2955).

DeLong JP, Hanson DT. 2009. Metabolic rate links density to demography in *Tetrahymena pyriformis*. ISME J 3:1396–401.

Deutsch CA, Tewksbury JJ, Huey RB, Sheldon KS, Ghalambor CK, Haak DC, Martin PR. 2008. Impacts of climate warming on terrestrial ectotherms across latitude. Proc Natl Acad Sci U S A105:6668–72.

Ernest SK, Enquist BJ, Brown JH, Charnov EL, Gillooly JF, Savage VM, White EP, Smith FA, Hadly EA, Haskell JP, Lyons SK, Maurer BA, Niklas KJ, Tiffney B. 2003. Thermodynamic and metabolic effects on the scaling of production and population energy use. Ecol Lett 6:990–5.

Feller G. 2010. Protein stability and enzyme activity at extreme biological temperatures. J Phys Condens Matter 22:323101.

Hobbs JK, Jiao W, Easter AD, Parker EJ, Schipper LA, Arcus VL. 2013. Change in heat capacity for enzyme catalysis determines temperature dependence of enzyme catalyzed rates. ACS Chem Biol 8:2388–93.

Hochachka PW, Somero GN. 2002. Biochemical adaption: mechanism and process in physiological evolution. Oxford: Oxford University Press.

Izem R, Kingsolver JG. 2005. Variation in continuous reaction norms: quantifying directions of biological interest. Am Nat 166:277–89.

Johnson FH, Lewin I. 1946. The growth rate of *E. coli* in relation to temperature, quinine and coenzyme. Comp Biochem Physiol A 141:1–7.

Kingsolver JG. 2009. The well-temperatured biologist. Am Nat 174:755–68.

Kingsolver JG, Diamond SE, Buckley LB. 2013. Heat stress and the fitness consequences of climate change for terrestrial ectotherms. Funct Ecol 27:1415–23.

Krenek S, Berendonk TU, Thomas P. 2011. Thermal performance curves of *Paramecium caudatum*: a model selection approach. Eur J Protistol 47:124–37.

Leroi AM, Bennett AF, Lenski RE. 1994. Temperature acclimation and competitive fitness: an experimental test of the beneficial acclimation assumption. Proc Natl Acad Sci U S A 91:1917–21.

Lindquist S, Craig EA. 1988. The heat-shock proteins. Ann Rev Genet 22:631–77.

Luhring TM, DeLong JP. 2016. Predation changes the shape of thermal performance curves for population growth rate. Curr Zool 62:501–5.

Luhring TM, Holdo RM. 2015. Trade-offs between growth and maturation: the cost of reproduction for surviving environmental extremes. Oecologia 178:723–32.

Novich RA, Erickson EK, Kalinoski RM, DeLong JP. 2014. The temperature independence of interaction strength in a sit-and-wait predator. Ecoshpere 5:137.

Overpeck J, Udall B. 2010. Dry times ahead. Science 328:1642–3.

Padfield D, Yvon-Durocher G, Buckling A, Jennings S, Yvon-Durocher G. 2016. Rapid evolution of metabolic traits explains thermal adaptation in phytoplankton. Ecol Lett 19:133–42.

Parmesan C, Yohe G. 2003. A globally coherent fingerprint of climate impacts across natural systems. Nature 421:37–42.

Parsell DA, Taulien J, Lindquist S. 1993. The role of heat-shock proteins in thermotolerance. Philos Trans R Soc Lond B Biol Sci 339:279–86.

Pauwels K, Stoks R, De Meester L. 2005. Coping with predator stress: interclonal differences in induction of heat-shock proteins in the water flea *Daphnia magna*. J Evol Biol 18:867–72.

Pörtner HO, Knust R. 2007. Climate change affects marine fishes through the oxygen limitation of thermal tolerance. Science 315:95–7.

Ratkowsky DA, Olley J, Ross T. 2005. Unifying temperature effects on the growth rate of bacteria and the stability of globular proteins. J Theor Biol 233:351–62.

Savage VM, Gillooly JF, Brown JH, West GB, Charnov EL. 2004. Effects of body size and temperature on population growth. Am Nat 163:429–41.

Scheiner SM. 2002. Selection experiments and the study of phenotypic plasticity. J Evol Biol 15:889–98.

Schoolfield RM, Sharpe PJH, Magnuson CE. 1981. Non-linear regression of biological temperature-dependent rate models based on absolute reaction-rate theory. J Theor Biol 88:719–31.

Schulte PM. 2015. The effects of temperature on aerobic metabolism: towards a mechanistic understanding of the responses of ectotherms to a changing environment. J Exp Biol 218:1856–66.

Schulte PM, Healy TM, Fangue NA. 2011. Thermal performance curves, phenotypic plasticity, and the time scales of temperature exposure. Integr Comp Biol 51:691–702.

Sharpe PJH, DeMichele DW. 1977. Reaction kinetics of poikilotherm development. J Theor Biol 64:649–70.

Vasseur DA, DeLong JP, Gilbert B, Greig HS, Harley CDG, McCann KS, Savage V, Tunney TD, O'Connor MI. 2014. Increased temperature variation poses a greater risk to species than climate warming. Proc R Soc B 281: 20132612.

Verity PG. 1985. Grazing, respiration, excretion, and growth rates of tintinnids. Limnol Oceanogr 30:1268–82.

Viant MR, Werner I, Rosenblum ES, Gantner AS, Tjeerdema RS, Johnson ML. 2003. Correlation between heat-shock protein induction and reduced metabolic condition in juvenile steelhead trout (*Oncorhynchus mykiss*) chronically exposed to elevated temperature. Fish Physiol Biochem 29:159–71.

Wilson RS, Franklin CE. 2002. Testing the beneficial acclimation hypothesis. Trends Ecol Evol 17:66–70.

Zamudio KR, Huey RB, Crill WD. 1995. Bigger isn't always better: body size, developmental and parental temperature and male territorial success in *Drosophila melanogaster*. Anim Behav 49:671–7.